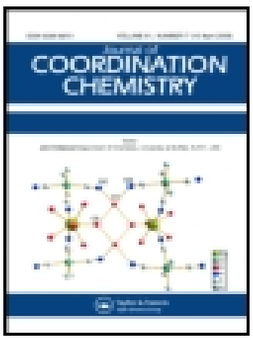

Journal of Coordination Chemistry

ISSN: 0095-8972 (Print) 1029-0389 (Online) Journal homepage: http://www.tandfonline.com/loi/gcoo20

The DNA-binding behavior and DFT calculation of ruthenium(II) complexes $[Ru(phen)_2L](ClO_4)_2$ (L = HMOPIP and MOHPIP)

Shao-Yu Liang, Yu-Xin Chen, Yong-Chang Zeng, Qiong Wu, Fanghua Qiu, Xin-Yu Wei, Li Li, Wen-Jie Mei & Wen-Jie Zheng

To cite this article: Shao-Yu Liang, Yu-Xin Chen, Yong-Chang Zeng, Qiong Wu, Fanghua Qiu, Xin-Yu Wei, Li Li, Wen-Jie Mei & Wen-Jie Zheng (2017): The DNA-binding behavior and DFT calculation of ruthenium(II) complexes $[Ru(phen)_2L](ClO_4)_2$ (L = HMOPIP and MOHPIP), Journal of Coordination Chemistry, DOI: 10.1080/00958972.2017.1411593

To link to this article: https://doi.org/10.1080/00958972.2017.1411593

Published online: 13 Dec 2017.

JOURNAL OF COORDINATION CHEMISTRY, 2017
https://doi.org/10.1080/00958972.2017.1411593

The DNA-binding behavior and DFT calculation of ruthenium(II) complexes $[Ru(phen)_2L](ClO_4)_2$ (L = HMOPIP and MOHPIP)

Shao-Yu Liang[a,b#], Yu-Xin Chen[c#], Yong-Chang Zeng[a], Qiong Wu[b], Fanghua Qiu[d], Xin-Yu Wei[e], Li Li[e], Wen-Jie Mei[e,f] and Wen-Jie Zheng[b]

[a]First Affiliated Hospital of Shenzhen University, Shenzhen, China; [b]School of Medicine, Jinan University, Guangzhou, China; [c]Department of Clinical Laboratory, School of Medicine, Shanghai Tenth People's Hospital, Tongji University, Shanghai, China; [d]Department of hospital infection control, Guangzhou Hospital of Traditional Chinese Medicine, Guangzhou, China; [e]School of Pharmacy, Guangdong Pharmaceutical University, Guangzhou, China; [f]Guangdong Province Engineering Technology Center for Molecular Probes & Biomedical Imaging, Guangzhou, China

ABSTRACT

Two ruthenium(II) complexes, $[Ru(phen)_2HMPIP]^{2+}$ (**1**) and $[Ru(phen)_2MHPIP]^{2+}$ (**2**), have been synthesized and characterized by elemental analysis, ESI-MS, and ^1H NMR spectroscopy. The DNA-binding properties of **1** and **2** have been investigated by electronic and emission spectra and viscosity experiments. The results show that both **1** and **2** can bind to DNA in intercalating mode, with **1** exhibiting stronger binding affinity. These were confirmed by the strong hypochromism at IL and MLCT absorption bands in both complexes when DNA was added into solution, and the increase in relative viscosity of CT-DNA in the presence of both complexes. Moreover, the calculated intrinsic binding constant for **1** and **2** from the decay of electronic spectra is 3.82×10^5 and 2.06×10^5 M^{-1}, respectively. Finally, the effects of the substituent groups on the DNA-binding behavior of ruthenium(II) complexes have also been rationally discussed by computer calculation of density functional theory (DFT) methods.

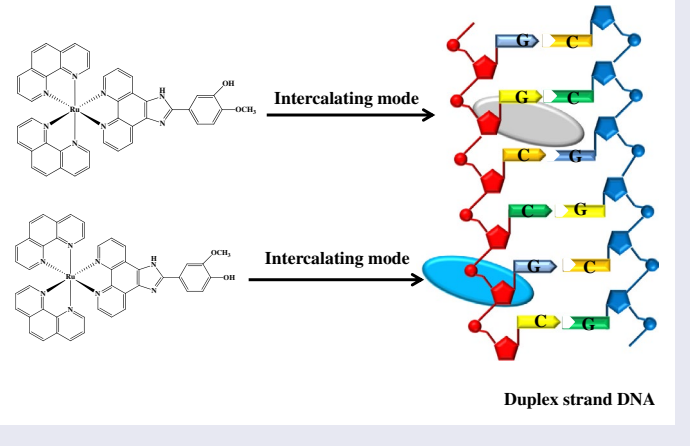

ARTICLE HISTORY
Received 19 August 2017
Accepted 18 November 2017

KEYWORDS
Ruthenium(II) complex; DNA-binding properties; HOMO; LUMO

CONTACT Fanghua Qiu qiufanghua1976@163.com; Wen-Jie Mei wenjiemei@126.com
#These authors contributed equally to the work.

1. Introduction

For years, the DNA-binding properties of ruthenium(II) complexes have been investigated for their potential utility on chemotherapy [1–5] and photodynamic therapy [6–9], because DNA molecules have long been considered as a common target for anticancer agents. In general, ruthenium(II) complexes have been reported to bind to DNA by three non-covalent binding modes including intercalation [10], groove-binding [11], and electrostatic binding mode [12–18]. In the last decade, a number of ruthenium(II) complexes have been designed and synthesized, and the assembling of these complexes with DNA has been investigated by all kinds of methods, such as UV and NMR spectroscopy and viscosity [19, 20]. These *in vitro* studies indicate that the binding mode and the binding affinity of ruthenium(II) complexes are dependent on the structure of DNA, as well as that of the structure of metal complexes [21–23]. It is shown that ruthenium(II) complexes with enlarged aromatic intercalating ligands and intramolecular hydrogen bond will bind to DNA with high affinity [24]. More recently, studies on the electron effect have shown that the electron-withdrawing group in intercalating ligand will improve the DNA-binding affinity of ruthenium(II) complexes [25, 26]. Nevertheless, the interaction of ruthenium(II) complexes with biological macromolecules is so complex, and to elucidate this is significant to design novel ruthenium(II) complexes with high biological activities.

Here, we report the synthesis of two ruthenium(II) complexes, $[Ru(phen)_2(HMPIP)]^{2+}$ (**1**) and $[Ru(phen)_2(MHPIP)]^{2+}$ (**2**) (Scheme 1). The DNA-binding properties of **1** and **2** have been investigated by spectroscopy and viscosity experiment. The results show that both complexes can bind to DNA in intercalative mode, the steric hindrance between methoxy group at intercalating ligand and the phosphor skeleton of DNA-helix play a key role to determine the binding affinity of these complexes with DNA molecules.

2. Experimental

2.1. Chemicals

Microanalyses were carried out on an Elementar Vario EL elemental analyzer. Electrospray experiments were carried out with a Thermo Finnigan LCQ DECA XP ion trap mass spectrometer, equipped with an ESI source. UV–Vis spectra were recorded on a Shimadzu UVPC-3000 spectrophotometer.

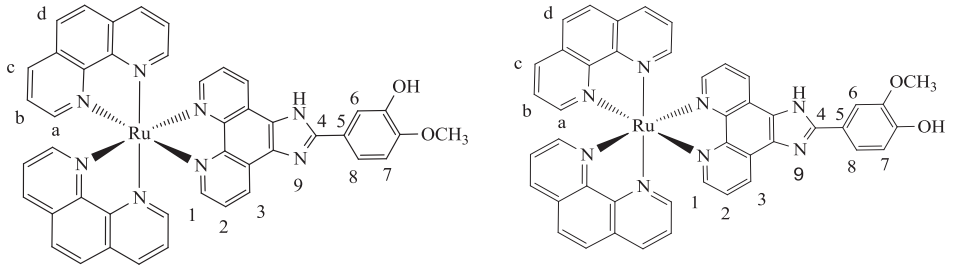

1 **2**

Scheme 1. The molecular structure of ruthenium(II) complexes $[Ru(phen)_2(HMPIP)]^{2+}$ (**1**) and $[Ru(phen)_2(MHPIP)]^{2+}$ (**2**).

2.2. Synthesis of (3-hydroxy-4-methoxy-phenyl)imidazo[4,5-f][1,10] phenanthroline) (HMPIP)

The ligand HMPIP was prepared as described [27] with some modification. In general, a solution of 1,10-phenanthraquinone (0.525 g, 2.5 mmol), ammonium acetate (3.88 g, 50 mmol), and 3-hydroxy-4-methoxyphenyl-aldehyde (532 mg, 3.5 mmol) in 10 mL glacial acetic acid was refluxed for 2 h. The cooled deep-red solution was diluted with 25 mL water and neutralized with ammonium hydroxide. Then, the mixture was filtered and the precipitates were washed with water and acetone, then dried and purified by chromatography over 60–80 mesh SiO_2 using absolute ethanol as eluent, and the obtained yield was 84% (753 mg). Calcd for $C_{27}H_{14}N_4O_4{\cdot}H_2O$: C, 68.1; H, 3.38; N, 11.8. Found: C, 67.8; H, 4.41; N, 11.2%.

2.3. Synthesis of (3-methoxy-4-hydroxy-phenyl)imidazo[4,5-f][1,10] phenanthroline) (MHPIP)

The ligand MHPIP was prepared by a similar method as above, but with 1,10-phenanthraquinone (525 mg, 2.5 mmol) and 3-methxoy-4-hydroxyphenyl-aldehyde (532 mg, 3.5 mmol); yield: 76% (685 mg). Calcd for $C_{27}H_{14}N_4O_4{\cdot}H_2O$: C, 68.1; H, 3.38; N, 11.8. Found: C, 67.8; H, 4.41; N, 11.2%.

2.4. Synthesis of $[Ru(phen)_2(HMPIP)](ClO_4)_2$ (1)

Ruthenium(II) complex **1** was synthesized as in the literature [28] with some modifications. $[Ru(phen)_2Cl_2]{\cdot}2H_2O$ (0.106 g, 0.20 mmol) and HMPIP (0.095 g, 0.20 mmol) were added to 10 cm^3 ethyleneglycol. The mixture was refluxed for 2 h under an argon atmosphere. The cooled reaction mixture was diluted with water (20 cm^3) and filtered to remove solid impurities. The complex was then separated from soluble impurities by precipitation with $NaClO_4$. The precipitated complex was dried, dissolved in a small amount of MeOH, and purified by chromatography over alumina oxide using MeOH-MeCN (10 : 1, v/v) as an eluent; yield: 67% (112 mg, calculated from $[Ru(phen)_2Cl_2]{\cdot}2H_2O$). Calcd for $C_{44}H_{34}Cl_2N_8O_{12}Ru$: C, 50.87; H, 3.30; N, 10.79. Found: C, 50.64; H, 3.45; N, 10.51%. ^{1}H NMR (DMSO-d_6, δ/ppm): 9.69(s, 1H); 9.05(dd, 2H); 8.76(d, 4H); 8.37(s, 4H); 8.13(d, 1H); 8.06(d, 2H); 7.99(d, 2H); 7.819(m, 7H); 7.03(7.001 d, 1H); 3.94(s, 3H). ^{13}C NMR (DMSO-d_6, δ/ppm): 153.64–153.50 (m), 153.35–153.16 (m), 153.16–152.96 (m), 150.43–150.15 (m), 147.72 (s), 147.64 (s), 147.62–147.07 (m), 137.28 (s), 130.92 (s), 128.54 (s), 126.81 (s), 122.92–122.28 (m), 120.01–119.11 (m), 119.19–118.18 (m), 116.36–115.08 (m), 114.90–113.43 (m), 113.43–111.89 (m). ESI-MS (in water, *m/z*): 901.0(14%) ($[M–ClO_4]^+$); 803.3(100%) ($[M–2ClO_4–H]^+$); 402.3 (28%) ($[M–2ClO_4]^{2+}$).

2.5. Synthesis of $[Ru(phen)_2(MHPIP)](ClO_4)_2$ (2)

Ruthenium(II) complex $[Ru(phen)_2(MHPIP)]^{2+}$ was synthesized as above, but with $[Ru(phen)_2Cl_2]{\cdot}2H_2O$ and MHPIP; yield: 72% (121 mg). Calcd for $C_{44}H_{34}C_{l2}N_8O_{12}Ru$: C, 50.87; H, 3.30; N, 10.79. Found: C, 50.68; H, 3.51; N, 10.31%. ^{1}H NMR (DMSO-d_6, δ/ppm): 9.41(s, 1H); 9.05(t, 2H); 8.76(d, 4H); 8.37(s, 4H); 8.12(t, 1H); 8.06(d, 2H); 7.98(d, 2H); 7.76(m, 7H); 7.19(d, 1H); 3.88 (s, 3H); ^{13}C NMR (DMSO-d_6, δ/ppm): 154.09–153.72 (m), 153.31–153.20 (m), 153.15–153.05 (m), 150.78–150.24 (m), 149.79–149.33 (m), 148.77–148.32 (m), 147.68

(d, $J = 9.0$ Hz), 137.27 (s), 130.93 (s), 128.54 (s), 126.86–126.71 (m), 126.54–126.40 (m), 120.68–120.58 (m), 116.57–116.36 (m), 111.15–110.92 (m). ESI-MS (in water, *m/z*): 901.0(16%) ($[M–ClO_4]^+$); 803.3(100%) ($[M–2ClO_4–H]^+$); 402.2(59%) ($[M–2ClO_4]^{2+}$).

2.6. Theoretical section

Both octahedral complexes $[Ru(phen)_2(HMPIP)]^{2+}$ and $[Ru(phen)_2(MHPIP)]^{2+}$ forms from Ru(II) and one main ligand or intercalating ligand L and two co-ligands (phen). There is no symmetry in these complexes. The full geometry optimization computations were performed for these complexes applying the DFT-B3LYP method [29–34] and LanL2DZ basis set [35, 36]. The structural modes of the studied compounds are shown in Scheme 1 and the singlet state was assumed [37]. All computations were performed with the G98 quantum chemistry program package [38]. In order to vividly depict the detail of the frontier molecular orbital interactions, the stereographs of some related frontier MO of the complexes were drawn with the Molden v3.6 program [39] based on the obtained computational results.

2.7. Absorption titration experiments

The electronic absorption spectra were recorded at room temperature to determine the binding affinity between DNA and polypyridyl ruthenium complexes. 3.0 mL solution of the blank buffer and the ruthenium complex were placed in the reference and sample cuvettes, respectively. During titration, an aliquot (2 μM) of buffered DNA solution was added to each cuvette to eliminate the absorbance of DNA itself. The titration processes were repeated until the spectra did not change for at least four titrations, indicating that binding saturation was achieved.

2.8. Fluorescence emission titrations

Fluorescence spectroscopy measurements were performed on an RF-5301 fluorescence spectrophotometer using a 1 cm path length quartz cell. Samples were excited at 340 nm and emission spectrum was recorded between 500 and 700 nm. After the solutions were mixed for 2 min, absorption spectra were recorded. The titration processes were repeated until there was no apparent change in the spectra for at least three titrations, indicating the achievement of the binding saturation [40].

2.9. Viscosity measurements

Viscosity measurements were carried out using an Ubbelodhe viscometer maintained at 32(± 0.1) °C in a thermostatic bath. Fixed solutions of complexes and DNA in different concentrations were prepared in Tris-HCl buffer medium, the DNA samples containing approximately 200 base pairs were used. The viscosity of DNA (η) was calculated by $\eta = t–t_0$, where t is flow times of DNA and t_0 is the flow times of bank (the Tris buffer solution). Flow times were measured by a digital stopwatch and each was measured three times. Viscosity of DNA are presented as $(\eta/\eta_0)^{1/3}$ *versus* binding ratio [41, 42], where η is the viscosity of DNA in the presence of complex and η_0 is the viscosity of DNA in the absence of complex [43].

3. Results

3.1. Synthesis and characterization

Ruthenium(II) complexes **1** and **2** were synthesized by refluxing the mixture of *cis*-$[Ru(phen)_2Cl_2]$ and corresponding ligands HMPIP and MHPIP, respectively. The complexes were obtained as ClO_4^- salts.

The ^{1}H NMR chemical shifts and their attribution of **1** and **2** are listed in Table 1. Compared to $[Ru(phen)_2(MHPIP)](ClO_4)_2$, the chemical shift at H_4 and $-OCH_3$ of $[Ru(phen)_2(HMPIP)](ClO_4)_2$ transfer to low field, while the chemical shift at H_5 transfer to high field.

3.2. DNA binding studies

Electronic spectra have been utilized to investigate the DNA-binding properties of **1** and **2**. At room temperature, both **1** and **2** exhibit an MLCT (metal-to-ligand charge-transfer) band at 458 nm and a strong IL (intra-ligand) band at 264 nm in the electronic spectra. In tris-HCl (pH = 7.2) buffer, the MLCT band of **1** shifts to 456 nm, while for **2** shifts to 453 nm. Upon addition of calf thymus DNA, the MLCT transition and IL transition bands of both **1** and **2** undergo obvious hypochromic effect and red-shift (Figure 1); the hypochromism for **1** and **2** are listed in Table 2.

Table 1. The chemical shift δ (ppm) of **1** and **2** and their attribution.

1		**2**	
δ (ppm)	Attribution	δ (ppm)	Attribution
9.692 (s, 1H)	H_6	9.408 (s, 1H)	H_6
9.048 (dd, 2H)	H_b	9.047 (t, 2H)	H_b
8.761 (d, 4H)	H_c	8.760 (d, 4H)	H_c
8.369 (s, 4H)	H_d	8.367 (s, 4H)	H_d
8.126 (d, 2H)	H_b	8.116 (t, 2H)	H_b
8.060 (d, 2H)	H_1	8.060 (d, 2H)	H_1
7.987 (d, 2H)	H_3	7.983 (d, 2H)	H_3
7.819 (m, 7H)	H_a, H_2, H_8	7.816 (m, 7H)	H_a, H_2, H_8
7.028 (d, 1H)	H_7	7.193 (d, 1H)	H_7
3.945 (s,3H)	$H(OCH_3)$	3.881 (s, 3H)	OCH_3

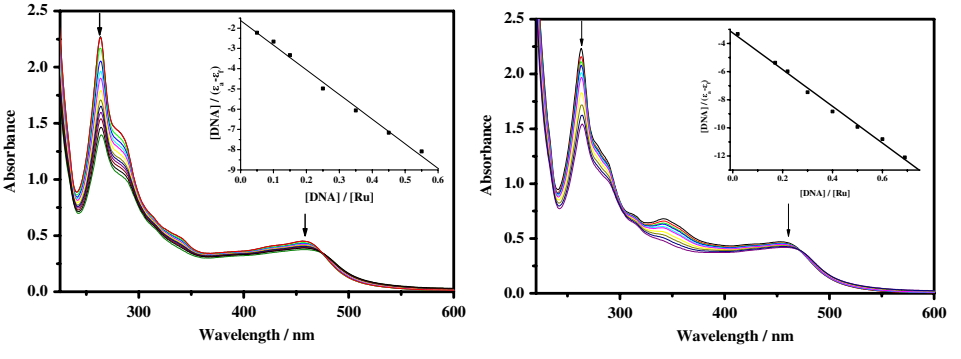

Figure 1. The electronic spectra of ruthenium(II) complexes **1** (left) and **2** (right) in the absence and presence of calf thymus DNA. [Ru] = 20 μM.

Table 2. The change of electronic spectra of ruthenium(II) complexes **1** (20 μM) and **2** (20 μM) in the absence and presence of calf thymus DNA.

	MLCT				IL			
Comp.	λ_0/nm	λ_b/nm	Δλ/nm	H/%	λ_0/nm	λ_b/nm	Δλ/nm	H/%
1	456	465	9	17	263	265	2	38
2	453	458	5	11	263	264	1	34

Notes: MLCT: metal to ligand charge transfer; IL: intra ligand charge transfer; H: hypochromism.

The intrinsic DNA-binding constants of ruthenium(II) complexes were calculated according to Equation (1):

$$\frac{[DNA]}{\varepsilon_a - \varepsilon_f} = \frac{[DNA]}{\varepsilon_b - \varepsilon_f} + \frac{1}{k_b(\varepsilon_b - \varepsilon_f)} \quad (1)$$

where [DNA] is the concentration of DNA in base pairs, ε_a, ε_f, and ε_b are the apparent extinction coefficient $\left(\frac{A_{obsd}}{[M]}\right)$, the extinction coefficient for free complex, and the extinction coefficient for the complex in the fully bound form, respectively. In plots of $\frac{[DNA]}{\varepsilon_a - \varepsilon_f}$ *versus* [DNA], K_b is given by the ratio of slope to intercept. The calculated binding constant for **1** and **2** is 3.82×10^5 and 2.06×10^5 M^{-1}, respectively, and are higher than those reported for polypyridine ruthenium(II) complexes in literature, with binding constants of 1.52×10^5–1.81×10^5 M^{-1} [44–48] and suggest that the increase of aromatic ring can improve the DNA-binding affinity. The calculated binding constants for $[Ru(phen)_2(o\text{-}TFPIP)]^{2+}$ (**1**) and $[Ru(phen)_2(p\text{-}CPIP)]^{2+}$ (**2**) are 5.81×10^4 and 8.55×10^4 M^{-1}, respectively.

3.3. Emission spectra

To further clarify the DNA-binding of **1** and **2**, the emission spectra of **1** and **2** were studied in the absence and presence of calf thymus DNA, as shown in Figure 2.

At room temperature, when excited at 470 nm, both **1** and **2** exhibit a strong emission band in range of 500–700 nm, with the maximum at 589 and 590 nm, respectively. When calf thymus DNA was added into solution, the emission observed decreased. At the [DNA]/[Ru] = 1.2, the I/I_0 for **1** and **2** is about 0.52 and 0.81, respectively (Figure 2(C)). These data are in agreement with that of electronic spectra, indicating that **1** binds more strongly than **2** to DNA due to the space hindrance when bound to DNA molecules.

3.4. Viscosity experiment

In order to elucidate the way ruthenium complex interacts with DNA, viscosity experiments give the strongest evidence to determine the binding mode of ruthenium(II) complexes to DNA in lacking of crystal data. In general, the relative viscosity of DNA will increase if a compound binds to DNA in an intercalative mode, while the groove-binding mode will decrease the relative viscosity of DNA resulting from the kink of double-strand helix of DNA. The relative viscosity of calf thymus DNA in the presence of **1** and **2** is shown in Figure 3.

Compared to $[Ru(bpy)_3]^{2+}$, which bind to DNA in electrostatic mode, the relative viscosity of calf thymus DNA increased in the presence of **1** and **2** because the space between base

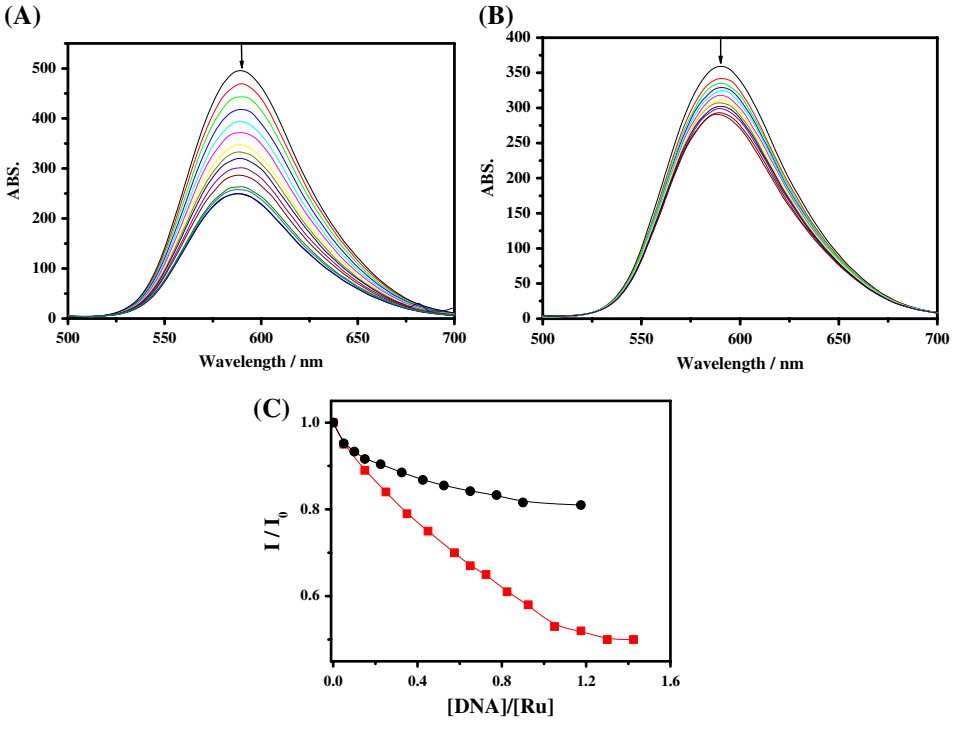

Figure 2. The emission spectra of ruthenium(II) complexes **1** (A) and **2** (B) in the absence and presence of calf thymus DNA. [Ru] = 20 μM. (C). The changes of emission of ruthenium(II) complexes **1** (■) and **2** (●) upon increasing amounts of calf thymus DNA.

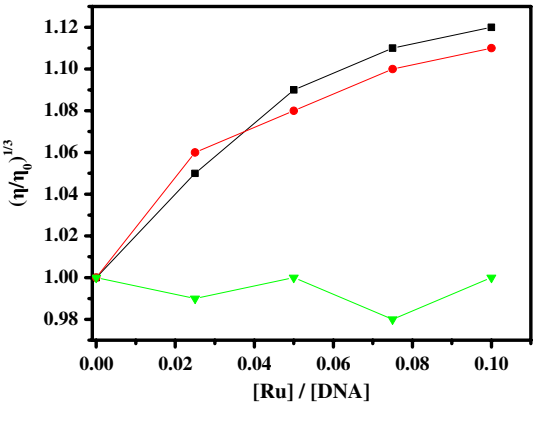

Figure 3. Effects of increasing amounts of Ru(II) complexes: $[Ru(phen)_2(HMPIP)]^{2+}$ **1** (■), $[Ru(phen)_2(MHPIP)]^{2+}$ **2** (●) and $[Ru(bpy)_3]^{2+}$ (▼) on the relative viscosity of CT-DNA in 5 mM Tris-HCl buffer (pH 7.2), 50 mM NaCl at 32(± 0.1) °C. [DNA] = 5.0×10^4 M.

pairs of double-stranded DNA helix is enlarged when the ligand of ruthenium(II) complex intercalates into base pairs. These data indicate that both **1** and **2** bind to DNA in intercalative mode.

4. Discussion

It is shown from spectroscopy and viscosity studies that both **1** and **2** can bind to DNA in intercalative mode, and **1** binds tighter than **2** to DNA. The theoretical computations by the DFT method were utilized to explain the fact, and the calculated bond lengths, bond angles, and dihedral angles of **1** and **2** are listed in Table 3.

According to Table 3, the dihedral angle (N9-C4-C5-C6) of **1** and **2** is 1.0 and 0.2°, respectively, indicating that **2** may bind to DNA more tightly than **1**, since the binding affinity of ruthenium(II) complexes depends on the planarity of intercalating ligands; this is in conflict with the results from the spectroscopy studies.

Based on the computation results, some frontier molecular orbital energies and total energies, the schematic diagram of the energies and related MLCT transitions, and the molecular orbital stereographs of $[Ru(phen)_2L]^{2+}$ are given in Table 4, Figure 4(B) and Figure 5, respectively.

As it is well established, there are π–π interactions in the DNA-binding of these complexes by intercalation mode. Kurita and Kobayashi [49] reported a simple calculation mode by the DFT method for stacked DNA base-pairs with backbones, and the computed HOMO and NHOMO (NH) energies of the DNA section mode with base pairs are much higher (−1.27 and −1.33 eV) than our computed LUMO and NLUMO (NL) energies (~ −7.0 eV) of complexes $[Ru(phen)_2L]^{2+}$ (L=HMPIP and MHPIP). We believe that such a trend in the relative energies will be retained in our DNA system, since the attraction of metal complex cations with high positive charges for electrons in MOs is much stronger than that of DNA, and thus the electron must easily be transferred from the HOMO of base pairs of DNA to the LUMO of the complexes intercalating to DNA [50, 51]. The LUMO energy of **1** and **2** is –0.2664 and –0.2667 a.u., respectively. Although the lower LUMO energy of **1** contributes to more binding affinity of this complex to DNA, the difference between **1** and **2** is so subtle to explain the difference in DNA-binding affinity of **1** and **2**.

There are other factors affecting the binding of these complexes with DNA. The calculated geometric structures of **1** and **2** are shown in Figure 4(A). From Figure 4(A), it is obviously different than the orientation of methoxy group in intercalating ligand. For **1**, the methoxy group is forward, which is apart from the phosphor skeleton when **1** approaches DNA molecules. At the same time, hydroxyl group at 3-position in HMPIP will form intramolecular hydrogen bond with the base pair of DNA helix to increase the DNA-binding affinity. As for

Table 3. The main bond lengths, bond angles, and dihedral angles of complexes **1** and **2**.

	Bond length/nm				Bond/ °		Dihedral angle/ °	
Comp.	$Ru–N_m$ [a]	$Ru–N_{co}$	$C–C(N)_m$ [b]	$C–C(N)_{co}$	A_m [c]	A_{co}	N9–C4–C5–C8	N9–C4–C5–C6
1	0.2105	0.2106	0.1405	0.1406	79.3	79.4	−179.0	1.0
2	0.2104	0.2106	0.1405	0.1406	79.3	79.5	−179.8	0.2

[a]$Ru–N_m$ expresses the mean coordination bond length between Ru and N atoms of the main ligand and Ru-Nco expresses that between Ru and N atoms of the coligand (phen).
[b]C–C(N)m expresses the mean bond length of the ring skeleton of the main ligand.
[c]Am expresses the coordination bond angle between Ru and two N atoms of the main ligand.

Table 4. Some frontier molecular orbits energies (ε_i/a.u) for ruthenium(II) complexes **1** and **2**.

Comp.	H–3	H–2	H–1	HOMO	LUMO	L+1	L+2	$\Delta\varepsilon_{L-H}$	$\Delta\varepsilon_{L-NH}$
1	−0.3945	−0.3915	−0.3715	−0.3371	−0.2664	−0.2630	−0.2597	0.0707	0.1051
2	−0.3951	−0.3919	−0.3746	−0.3416	−0.2667	−0.2633	−0.2600	0.0749	0.1079

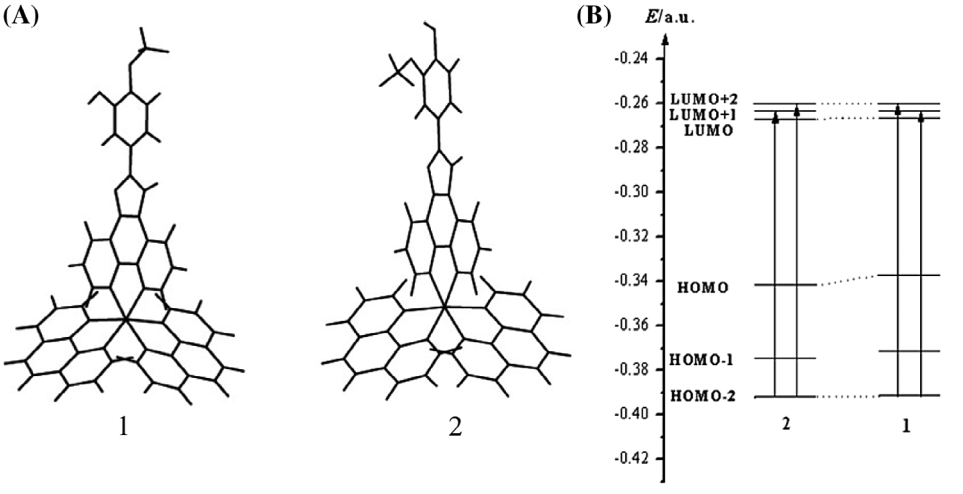

Figure 4. (A) Calculated geometric structures of ruthenium(II) complexes **1** and **2**. (B) Schematic diagrams of some frontier MO energies and the related MLCT transitions of complexes **1** and **2**.

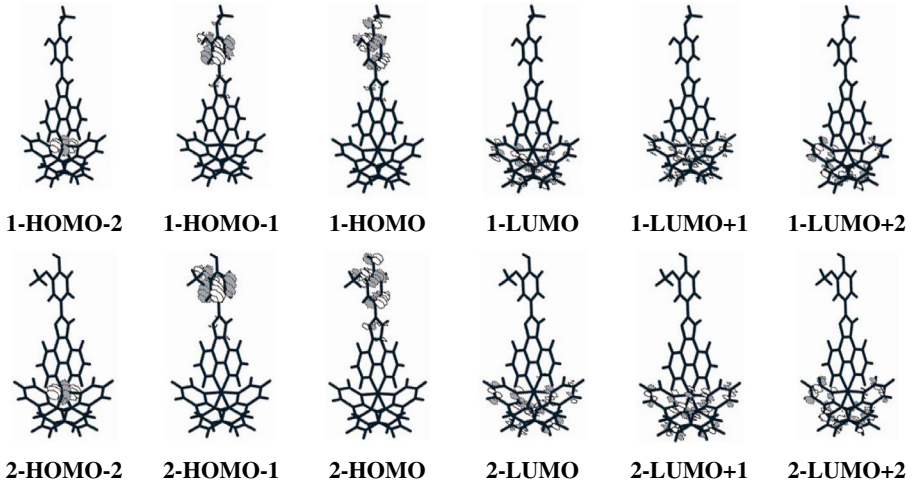

Figure 5. Some related frontier MO stereographs of ruthenium(II) complexes **1** and **2**.

2, although the hydroxyl group is at 4-position in intercalating ligand to improve the binding affinity of this complex with DNA, the repulsion force between the methoxy group at 3-position in MHPIP and the phosphor skeleton of double-stand DNA will distort MHPIP to destroy the planarity of this ligand when **2** interacts with DNA. As a result, the steric hindrance between the intercalating ligand and DNA will decrease the binding affinity of **2**.

5. Conclusion

Two ruthenium(II) complexes, $[Ru(phen)_2(HMPIP)]^{2+}$ (**1**) and $[Ru(phen)_2(MHPIP)]^{2+}$ (**2**), have been synthesized by refluxing *cis*-$[Ru(phen)_2Cl_2]$ and corresponding ligands HMPIP and

MHPIP under Ar atmosphere. These complexes have been characterized by elemental analysis, ESI-MS, and ^{1}H NMR spectroscopy. The investigation on the DNA-binding properties of **1** and **2** by spectroscopy and viscosity techniques show that both complexes bind to DNA in intercalative mode. The intrinsic DNA-binding constants calculated for **1** and **2** are 3.82×10^5 and 2.06×10^5 M^{-1}, respectively. The emission spectra increased in the presence of CT-DNA, and the relative emission strength for **1** and **2** at ratio of [DNA]/[Ru] = 1.2 is *ca.* 0.52 and 0.81, respectively. These data, together with the results of electronic spectra, show that **1** binds more strongly than **2** to DNA.

In general, there are three factors determining the binding affinity of ruthenium(II) complexes and DNA; that is the planarity of intercalating ligand, the frontier molecular orbits energies, and the steric hindrance between the substituent group at intercalating ligand and the phosphor skeleton of double-stranded DNA-helix. The studies on the calculation by DFT methods show that the steric hindrance play a key role in the interaction of ruthenium(II) complexes $[Ru(phen)_2(HMPIP)]^{2+}$ and $[Ru(phen)_2(MHPIP)]^{2+}$, and the detailed mechanism is under further investigation.

Disclosure statement

No potential conflict of interest was reported by the authors.

Funding

This work was supported by the National Nature Science Foundation of China [grant number 81572926], [grant number 81603669]; the Provincial Major Scientific Research Projects in Universities of Guangdong Province [grant number 2014KZDXM053]; the Science and Technology Project of Guangdong Province [grant number 2014A020212312]; Natural Science Fund of Guangdong [grant number 408182136045]; the Science Foundation for China Postdoctor [grant number 2016M592604].

References

[1] S.M. Guichard, R. Else, E. Reid, B. Zeitlin, R. Aird, M. Muir, M. Dodds, H. Fiebig, P.J. Sadler, D.I. Jodrell. *Biochem. Pharmacol.*, **71**, 408 (2006).
[2] F. Pierard, A. Kirsch-De Mesmaeker. *Inorg. Chem. Commun.*, **9**, 111 (2006).
[3] F. Schmitt, P. Govindaswamy, G. Süss-Fink, W.H. Ang, P.J. Dyson, L. Juillerat-Jeanneret, B. Therrien. *J. Med. Chem.*, **51**, 1811 (2008).
[4] E. Wachter, D.K. Heidary, B.S. Howerton. *Chem. Commun.*, **48**, 9649 (2012).
[5] M. Brindell, E. Kuliś, S.K. Elmroth, K. Urbańska, G. Stochel. *J. Med. Chem.*, **48**, 7298 (2005).
[6] W.J. Mei, J. Liu, K.C. Zheng, L.J. Lin, H. Chao, A.X. Li, F.C. Yun, L.N. Ji. *Dalton Trans.*, 1352 (2003).
[7] H. Chao, W.J. Mei, Q.W. Huang, L.N. Ji. *J. Inorg. Biochem.*, **92**, 165 (2002).
[8] K. Qiu, J. Wang, C. Song, L. Wang, H. Zhu, H. Huang, J. Huang, H. Wang, L. Ji, H. Chao. *ACS Appl. Mater. Inter.*, **9**, 18482 (2017).
[9] W. Sun, S. Li, B. Häupler, J. Liu, S. Jin, W. Steffen, U.S. Schubert, H.-J. Butt, X.-J. Liang, S. Wu. *Adv. Mater.*, **29**, 1603702 (2017).
[10] C.J. Cardin, J.M. Kelly, S.J. Quinn. *Chem. Sci.*, **8**, 4705 (2017).
[11] J.P. Hall, P.M. Keane, H. Beer, K. Buchner, G. Winter, T.L. Sorensen, D.J. Cardin, J.A. Brazier, C.J. Cardin. *Nucleic Acids Res.*, **44**, 9472 (2016).
[12] X.H. Zou, B.H. Ye, H. Li, J.G. Liu, Y. Xiong, L.N. Ji. *Dalton Trans.*, 1423 (1999).
[13] L. Ji, Q. Zhang, C. Hui, L. Ji, Q. Zhang, C. Hui. *Sci. China*, **46**, 1332 (2001).
[14] P.L. And, B. Nordén. *J. Phys. Chem. B*, **102**, 9583 (1998).
[15] Y. Xiong, L.N. Ji. *Coord. Chem. Rev.*, **185**, 711 (1999).

[16] J.G. Liu, B.H. Ye, H. Li, L.N. Ji, R.H. Li, J.Y. Zhou. *J. Inorg. Biochem.*, **73**, 117 (1999).
[17] W.J. Mei, Y.Z. Ma, J. Liu, J.C. Chen, K.C. Zheng, L.N. Ji, J.H. Yao. *Transition Met. Chem.*, **31**, 277 (2006).
[18] N.M. Gabra, B. Mustafa, Y.P. Kumar, C.S. Devi, A. Srishailam, P.V. Reddy, K.L. Reddy, S. Satyanarayana. *J. Fluoresc.*, **24**, 169 (2014).
[19] Y. Sun, J. Li, H. Zhao, L. Tan. *J. Inorg. Biochem.*, **163**, 88 (2016).
[20] D. Lazić, A. Arsenijević, R. Puchta, Ž.D. Bugarčić, A. Rilak. *Dalton Trans.*, **45**, 4633 (2016).
[21] S. Fukuzumi, M. Tanaka, M. Nishimine, K. Ohkubo. *J. .Photochem. Photobiol. A: Chem.*, **175**, 79 (2005).
[22] K.K. Naresh, R. Ramesh, Y. Liu. *J. Inorg. Biochem.*, **100**, 18 (2006).
[23] E. Ioachim, E.A. Medlycott, G.S. Hanan, F. Loiseau, S. Campagna. *Inorg. Chim. Acta*, **359**, 766 (2006).
[24] R.P. Paitandi, R.S. Singh, S. Mukhopadhyay. *Inorg. Chim. Acta*, **454**, 117 (2016).
[25] J. Liu, W.J. Mei, L.J. Lin, K.C. Zheng, H. Chao, F.C. Yun, L.N. Ji. *Inorg. Chim. Acta*, **357**, 285 (2004).
[26] H. Luo, J. Xiao, J. Chen, H. Xu, J. Lu, Z. Liu, S. Chen, M. Tong, K. Zheng, L. Ji. *Chin. J. Chem.*, **28**, 1317 (2010).
[27] E.A. Steck, A.R. Day. *J. Am. Chem. Soc.*, **65**, 121 (1943).
[28] R. Hage, J.G. Haasnoot, J. Reedijk, R. Wang, E.M. Ryan, J.G. Vos, A.L. Spek, A.J.M. Duisenberg. *Inorg. Chim. Acta*, **174**, 77 (1990).
[29] P. Hohenberg, W. Kohn. *Phys. Rev. B*, **136**, B864 (1964).
[30] A.D. Becke. *J. Chem. Phys.*, **98**, 1372 (1993).
[31] A. Görling. *Phys. Rev. A*, **46**, 3753 (1992).
[32] R. Behjatmanesh-Ardakani, F. Pourroustaei-Ardakani, M. Taghdiri. *J. Mol. Model.*, **22**, 3 (2016).
[33] V. Dixit, R.A. Yadav. *Int. J. Pharm.*, **491**, 277 (2015).
[34] R. Behjatmanesh-Ardakani. *Struct. Chem.*, **25**, 919 (2014).
[35] P.J. Hay, W.R. Wadt. *J. Chem. Phys.*, **82**, 270 (1985).
[36] M. Khajehzadeh, M. Moghadam. *Spectrochim. Acta, Part A*, **180**, 51 (2017).
[37] A. Juris, V. Balzani, F. Barigelletti, S. Campagna, P. Belser, A.V. von Zelewsky. *Coord. Chem. Rev.*, **84**, 85 (1988).
[38] M. Frisch. *J. Am. Chem. Soc.*, **24**, 235 (1998).
[39] J. Wang, X. Hou, Z. Zhao, H. Bo, Q. Chen. *Inorg. Chem. Commun.*, **67**, 40 (2016).
[40] W.J. Mei, Y.X. Liu, J. Liu, J. Li, K.C. Zheng, L.N. Ji. *Transition Met. Chem.*, **30**, 82 (2005).
[41] Q. Wu, J. Wu, W.-J. Mei, Q. Wang, Z. Zhang, X.-H. Wu, F.-Y. Sun, W.-L. Wu, Y.-H. Chen, X.-Y. Hu, Y.-Y. Tao. *Aust. J. Chem.*, **66**, 1422 (2013).
[42] G. Cohen, H. Eisenberg. *Biopolymers*, **8**, 45 (1969).
[43] H. Fritzsche, H. Triebel, J.B. Chaires, N. Dattagupta, D.M. Crothers. *Biochem.*, **21**, 3940 (1982).
[44] C. Wang, Q. Wu, Y. Zeng, D. Huang, C. Yu, X. Wang, W. Mei. *J. Coord. Chem.*, **68**, 1489 (2015).
[45] S. Sathiyaraj, R.J. Butcher, C. Jayabalakrishnan. *J. Coord. Chem.*, **66**, 580 (2013).
[46] P. Čanović. *J. Biol. Inorg. Chem.*, **43**, 1 (2017).
[47] R.R. Mallepally. *J. Fluoresc.*, **27**, 1 (2017).
[48] P.V. Reddy. *Anal. Biochem.*, **485**, 49 (2015).
[49] N. Kurita, K. Kobayashi. *Comput. Chem.*, **24**, 351 (2000).
[50] K. Fukui, T. Yonezawa, H. Shingu. *J. Chem. Phys.*, **20**, 722 (2004).
[51] R. Misra, P. Gautam. *Org. Biomol. Chem.*, **12**, 5448 (2017).